International Journal of Renewable Energy Resources 12 (2022) 42-58
https://doi.org/10.22452/ijrer.vol12no2.1

IMPACT OF TEMPERATURE AND REACTION TIME ON THE CONVERSION OF POLYSTYRENE WASTE TO PYROLYTIC OIL AND ITS DIESEL ENGINE PERFORMANCE, EMISSION, AND LUBRICITY CHARACTERISTICS

Muhamad Sharul Nizam Awang[1*], Nurin Wahidah Mohd Zulkifli[1,2*], Muhammad Mujtaba Abbas[1,3], Syahir Amzar Zulkifli[1], Mohd Nur Ashraf Mohd Yusoff[1], Muhammad Hazwan Ahmad[4], Wan Mohd Ashri Wan Daud[5], Md Abul Kalam[1,2]

[1]Department of Mechanical Engineering, Faculty of Engineering, University of Malaya, 50603 Kuala Lumpur, Malaysia
[2]Center for Energy Sciences (CFES), Department of Mechanical Engineering, Faculty of Engineering, University of Malaya, 50603 Kuala Lumpur, Malaysia
[3]Department of Mechanical, Mechatronics and Manufacturing Engineering (New Campus), University of Engineering and Technology Lahore, Lahore 54000, Pakistan
[4]Institute for Advanced Studies, University of Malaya, 50603 Kuala Lumpur, Malaysia
[5]Department of Chemical Engineering, Faculty of Engineering, University of Malaya, 50603 Kuala Lumpur, Malaysia
*e-mail: nizamawang95@gmail.com; nurinmz@um.edu.my

Abstract
The focus of this research is to see how temperature and reaction time affect the yield and quality of liquid oil obtained by pyrolysis. In a small batch of pyrolysis reactor/small pyrolysis reactor batch, polystyrene waste was employed as a feedstock. There are limited studies on utilizing polystyrene waste pyrolytic oil (PWPO) for diesel engine applications. Therefore, this study studied the performance and emission characteristics of liquid oil produced at optimal condition (PS100). This study is the first to look into the impact of polystyrene waste pyrolysis oil on the lubricity of the fuel. In addition, this study also focused on lubrication degradation caused by dilution using PWPO, which had never been done previously. The ideal temperature and reaction time were discovered to be 400 °C and 30 min, where the liquid oil yield was amounted at 92.94% by mass. PS100 had similar properties to commercial diesel. PS100 comprises of 34.6% aromatics, 25.2% alkanes, and 4.3% alkenes. PS100 delivered superior performance than B10 diesel. The brake thermal efficiency, brake power, and brake torque were up by 15.5, 5.6, and 2.38%, respectively, while the brake-specific fuel consumption was down by 8.00%. PS100 emitted 97.06 and 17.3% more hydrocarbon and carbon dioxide than B10, respectively. Its poor exhaust gas emissions have proven a key stumbling block in its application in diesel engine. PS100 demonstrated 27.6% increase in coefficient of friction and 29.8% increase in lubricant contamination as compared to B10. Despite its low lubricity and emissions, PS100 has a lot of potential as a diesel engine alternative fuel.

Keywords: Polystyrene Waste; Pyrolysis; Diesel Engine; Performance; Exhaust Gas Emission; Lubricity; Lubricant Dilution

1. INTRODUCTION

Global consumption of energy constantly rises to keep up with human demand since the beginning of the industrial revolution. Due to the growing population and the rapid economic growth of developing countries, energy consumption is not anticipated to decline in the twenty-first century (Mujtaba et al., 2020a). Fig. 1 depicts the global and Malaysian yearly amounts of plastic waste. About 359 million tonnes of plastic waste were produced worldwide year-round in 2018. Plastic waste is expected to grow by 19% to 444 million tonnes in 2025, compared to 2018. In 2018, Malaysia produced about 1.83 million tonnes. Malaysia's plastic waste output would increase by 13% to 2.09 million tonnes by 2025, compared to 2018. Plastic waste is a preferable alternative to be converted into fuel because of its cost-effectiveness and great availability in Malaysia, provided that it is managed appropriately. Polystyrene is a popular non-recyclable material that accounts for 13% of Malaysia's plastic waste. Polystyrene is not recycled since it is easily blown away and creates garbage during the collecting process due to its lightness. Furthermore, because of its high shipping costs, polystyrene is not chosen owing to its bulkiness. Thus, polystyrene waste was chosen as a pyrolysis feedstock in this study.

Future energy needs are expected to be met by alternative fuels as fossil fuel supplies gradually

decline (Rizwanul Fattah et al., 2020). Researchers particularly agreed that the pyrolysis oil from plastic waste to alleviate energy crises because it has a high utilization rate and the potential to become an alternative fuel. In terms of volume, most studies claim that pyrolysis of plastic waste produces a considerable amount of liquid (greater than 80% by weight) (Damodharan et al., 2019; Singh et al., 2019). The calorific value, viscosity and flash point of waste plastic pyrolytic oil (WPPO) is comparable to diesel among alternative fuels. Most studies assert that pyrolysis of plastic waste results in the production of a sizeable amount of liquid (more than 80% by weight) in terms of volume. Waste plastic pyrolytic oil (WPPO) is one of the alternative fuels that is most comparable to diesel in terms of viscosity, flash point, density, and calorific value.

However, WPPO has a pour point of less than -15°C (Khan et al., 2016). Because of its low pour point, it is difficult to use in areas with cold temperatures. Plus, its low pour point would not be a big concern in Malaysia, in which it can perform satisfactorily year-round because of its tropical weather year round and its low temperature is between 18 – 25ºC (Wong et al., 2022). Because WPPO has properties similar to diesel, several studies have been directed at using it in diesel engines (Damodharan et al., 2017). According to the literature, diesel engines running on WPPO deliver consistent performance and efficiency (Kaimal & P, 2015). Despite having a lower viscosity (2.9 cSt) than diesel (3.1 cSt), when WPPO is burnt, the tiny droplets are produced during atomization for optimal combustion (Singh et al., 2020). As a result, WPPO aids in the improvement of the brake-specific fuel consumption (BSFC) (Singh et al., 2020). WPPO had a brake thermal efficiency (BTE) that was approximately 5% higher than diesel (Sachuthananthan et al., 2018, Kaewbuddee et al., 2020). In contrast, WPPO is quickly becoming one of the finest alternative fuels, as it improves the performance of diesel engines.

Nonetheless, Kalargaris et al. (2017a) and Mani et al. (2011) reported that WPPO emitted more hydrocarbon (HC) and nitrogen oxide (NO_x) than diesel, . They studied the exhaust emissions from diesel engines that were running on various blends of diesel and WPPO. Moreover, Mani et al. examined the effect of blank WPPO in single-cylinder engines. They found that carbon monoxide (CO), NOx, and smoke emissions rose by 5, 25, and 40%, respectively, when compared to diesel. Higher CO emissions could also be due to the radicals produced by the breakdown of high molecular weight and complex molecules in the fuel react with one another, forming polymers by condensation at higher temperatures. These carbon-like structured polymers accumulate in the combustion chamber and obstruct optimal combustion (Kumar et al., 2016). Despite that, Kumar et al. (2016) and Kalargaris et al. (2017a) reported that the WPPO had a high aromatics' content, which decreased HC by 43.8 and 85.1%, respectively, when compared to diesel. Researchers should be aware that adding WPPO to fuel blends raises exhaust gas emissions in general.

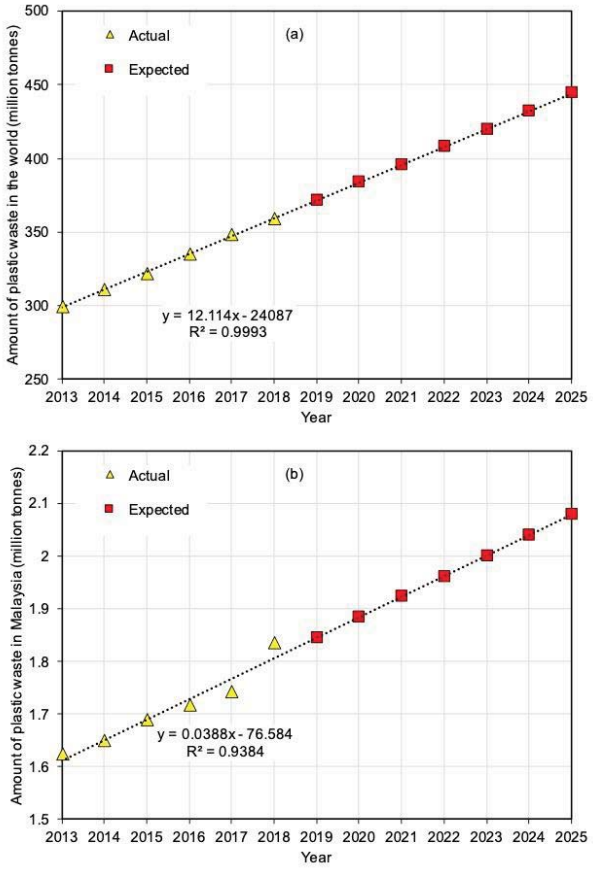

Fig.1 (a) Global and (b) Malaysia production of plastic waste (Kin & Jasmin, 2019).

The majority of diesel engine components, such as the injector and fuel pump, self-lubricate. Diesel has very poor lubricity because desulfurization removes polar molecules (Gul et al., 2020). Lubricity is essential for improving the overall effectiveness of engine parts (Awang et al., 2021). As a result, several researchers advocated for the use of WPPO in engines to boost diesel lubricity. According to Awang et al. (2020), adding WPPO to diesel (10 to 50% WPPO) reduced the coefficient of friction (COF) average. Long-chain polymer base oils enhanced the lubricity by decreasing friction (Awang et al., 2022). Therefore, the WPPO could be a potential replacement fuel of diesel fuel to provide better lubricity. Overall, WPPO has a beneficial influence on diesel engine performance characteristics, according to the previous research. Furthermore, it is a promising alternative fuel with good lubricity properties. There are limited studies on utilizing

polystyrene waste pyrolytic oil (PWPO) for diesel engine applications, according to the literature study. Few studies on the tribological properties of WPPO fuel have been published, and some of them only offer the average change in COF and wear scar diameter (WSD), which is inadequate to fully explain the fuel's lubricity. As a consequence, the influence of WPPO on the tribological properties of diesel engine part was comprehensively investigated in this study. It is unknown how PWPO pollution affects commercial lubricant. Additionally, the alteration in engine oil properties is not emphasised. It is essential because contamination of the lubricant will reduce engine lifetime (mixed pyrolysis oil). Therefore, this research also explored the lubrication degradation induced by WPPO dilution, which had never been done before.

Polystyrene was utilized as a raw material in this study to examine the liquid yield and by-product generation throughout the pyrolysis. Additionally, by employing liquid as the primary product and gas and char as the by-products, the energy recovery is evaluated. The impact of temperature and reaction time on the quantity and quality of liquid oil produced during pyrolysis was studied. The chemical composition and physicochemical properties of the liquid oil generated were also determined. The potential of liquid oil as a transportation fuel was investigated in depth based on these characterization results. Apart from optimizing the production of PWPO, the goal of this work is to (1) study the performance, emission, and lubricity characteristics of PWPO, which is used to improve overall engine characteristics, and (2) investigate the impact of PWPO on the tribological performance of mineral lubricants.

2. MATERIALS AND METHODS

2.1. MATERIALS

The polystyrene plastic samples were collected from a Malaysian post-consumer polymer waste stream. To eliminate contaminants and moisture, the plastic samples were washed and dried in a 100°C oven overnight. The dried plastic waste was chopped and used as a raw material to the reactor. B10 was bought at a local petrol station. AISI 52100 Chrome hard polished steel balls with a diameter of 6.2 mm, 15-mm SAE-AMS 6440 steel smooth diamond polish discs, and 12.7-mm-diameter AISI 52100 steel balls with a hardness of 64–66 Rc were purchased from the local supplier in line with ASTM D6079-11 specifications.

2.2. PWPO PRODUCTION

To pyrolyze the plastic waste, a small-scale batch reactor was developed (Fig.2). An internally manufactured glass reactor (with a capacity of 500 mL), nitrogen cylinder, tube condenser with water cooler, pump, collecting flask, and heating mantle with stirrer (with a maximum temperature of 450°C) make up the entire equipment. In each experiment, 100 g of raw materials were utilized. To create an inert environment, nitrogen gas at a pressure of 5 L/min was vented into the reactor for 10 s before the reaction began. The reactor was heated to 300°C. The feed material was transformed into organic vapor, which was condensed into liquid oil and collected in the flask after passing through the condenser. To achieve maximal condensation of organic vapor, a LabTech chiller was utilized to keep the condenser temperature below 10°C, with a coolant flow rate of 30 L/min. The reaction time was measured from the first drop of liquid oil generated. When the system had cooled to ambient temperature, the residue (char) was collected at the end of each experiment. After each experiment, the mass balance of products was calculated by weighing the amount of liquid oil and coke, and the remaining 100% weight percentages were assumed to be gas products. The reaction was done three times for each parameter.

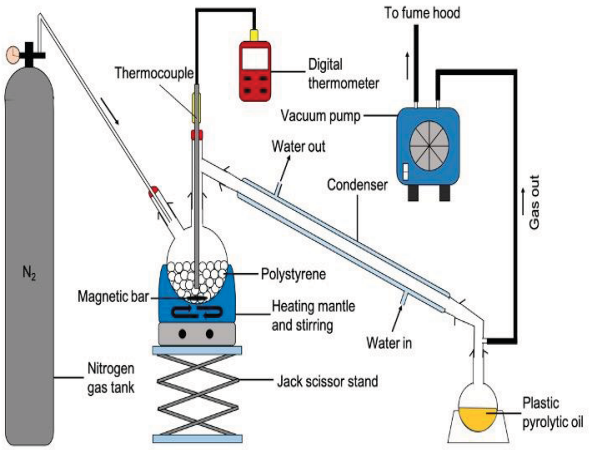

Fig.2 Small scale batch pyrolysis reactor.

2.3. CHARACTERIZATION OF FEEDSTOCK, PWPO AND B10

Thermogravimetric analysis (TGA) of polystyrene plastic was performed by Mettler Toledo TGA (SDTA851), which tracked the thermal behaviour of raw materials under controlled circumstances to determine the best process temperature and reaction time. Under nitrogen flow, a 10 g sample was put into an alumina crucible and heated at 50 ml/min at a rate of 10°C/min from 25 to 900°C. Standard ASTM techniques were used to characterize the PWPO and B10. To compare the PWPO's properties to B10 diesel, the viscosity (kinematics), density, and calorific value of liquid oil were studied. The viscosity and density of liquid oil

were measured using a Discovery Hybrid rheometer (HR1 of the TA equipment). The calorific value of PWPO and B10 was determined using the bomb calorimeter. Using PWPO that was produced at the optimal parameters (PS100), the fuel lubricity and the characteristics of the diesel engine were studied (PS100). PS100 fuel was compared to B10 diesel. Table 1 lists the PS100 and B10's physicochemical properties. Standard methods (ASTM D6751 and EN 14214) were applied to determine the physicochemical properties of the fuels.The composition of PS100 and B10 was determined using gas chromatography-mass spectrometry (GC-MS). TheNsample was introduced into the chromatographic inlet and processed for 42 min after 50 mg of the liquid fuel product was dissolved in 1 mL of n-hexane. Helium is utilized as the carrier gas, and the flow rate is 0.51 mL/min. The separation began at a temperature of 50 to 250°C with a 5°C/min heating rate (Juwono et al., 2018).

2.4. LUBRICANT SAMPLE PREPARATION

5% of fuel samples were blended with commercial SAE-40 lubricant at 900 rpm for 30 min, because the lubricant mixture with the fuel was resulted at only 5% due to crankcase dilution (Mujtaba et al, 2020b). A viscometer (SVM 3000) was used to determine the physicochemical properties of SAE-40 reference lubricant and all other lubricant samples with various fuels, as shown in Table 2.

2.5. EXPERIMENTAL SET UP

2.5.1. Diesel engine set up

In this study, a diesel engine test bed (model: Yanmar (TF 120 M)) from the University Malaya was used to investigate diesel engine parameters for various fuel samples. Fig.3 and Table 3 show the schematic view of diesel engine set-up and its specifications, respectively.

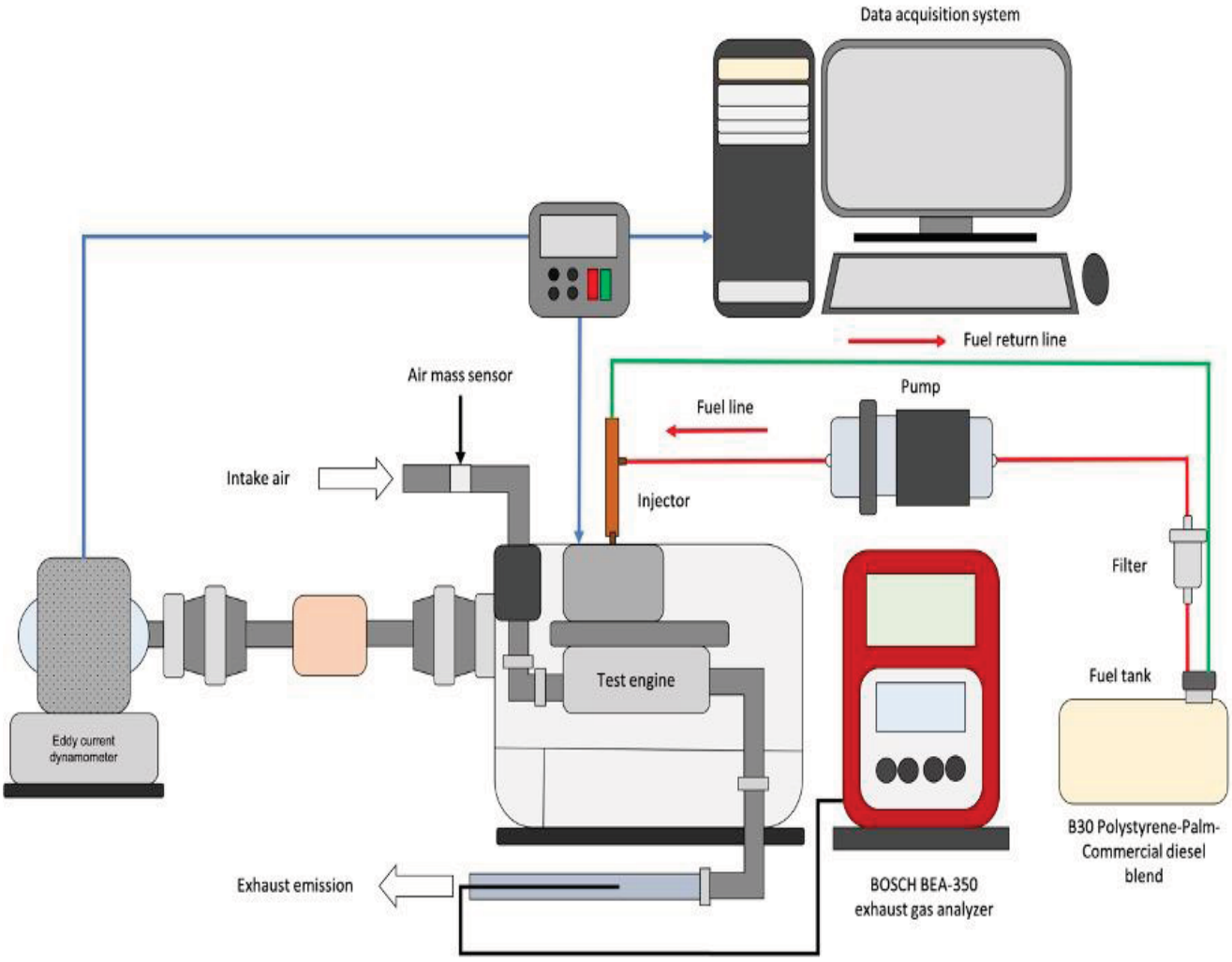

Fig.3 Schematic view of diesel engine set-up.

Table 1: Physicochemical properties of tested fuel samples.

Test fuels	Density at 15°C	Kinematic viscosity at 40°C	Kinematic viscosity at 100°C	Dynamic viscosity at 40°C	Dynamic viscosity at 100°C	Calorific value	Viscosity index
	kg/m^3	mm^2/s	mm^2/s	mPa.s	mPa.s	MJ/kg	
PS100	0.9388	1.4302	0.7294	1.3130	0.6332	43.5080	57.6
B10	0.8485	3.1757	1.2816	2.6375	1.0092	46.5677	156.17

Table 2: Physicochemical properties of tested lubricant fuel samples.

Lubricant samples	Density at 15°C	Kinematic viscosity at 40°C	Kinematic viscosity at 100°C	Dynamic viscosity at 40°C	Dynamic viscosity at 100°C	Viscosity index
	kg/m^3	mm^2/s	mm^2/s	mPa.s	mPa.s	
100% Lubricant (SAE 40)	898.0	130.58	13.40	114.67	11.13	97.0
Lubricant + 5% PS100	896.1	82.56	10.33	72.66	8.69	107.1
Lubricant + 5% B10	895.4	129.44	11.62	113.68	9.73	70.0

Table 3: Engine specifications used for experimental work.

Engine specification	Description
No. of cylinders	1
Aspiration	Radiator cooling
Cylinder bore × stroke (mm)	92 × 96
Displacement (L)	0.638
Compression ratio	17.7
Maximum engine speed (rpm)	2400
Maximum power (kW)	7.7
Injection timing (deg.)	17° BTDC
Injection pressure (kg/cm^2)	200
Power take-off position	Flywheel side
Cooling system	Radiator cooling
Connecting rod length (mm)	149.5

The B10 diesel flow rate was monitored to determine the characteristics of the internal combustion engine. Utilizing a graduated measuring cylinder, three measurements and their average per 10 ml of fuel samples were recorded at each engine speed evaluated. Meanwhile, a timer was used to keep track of the passing time. The brake torque (BT) and brake power (BP) were then analyzed using the (DAPSTEP8) software. The exhaust gas emissions (HC, CO, and carbon dioxide (CO_2)) measured by a BOSCH gas analyzer are summarized in Table 4. However, owing to the gas analyzer's limitations, NO_x could not be measured.

Firstly, a diesel engine was utilized to operate the B10 fuel sample in order to keep the procedure under control. The diesel engine was then filled with PS100 fuel to examine the engine's characteristics. The test rig diesel engine was operated at six different speeds (900, 1200, 1500, 1800, 2100, and 2400 rpm) at full load. The relative uncertainty percentages for the engine parameters (BSFC, BP, BTE, CO, HC, and CO_2) were computed using different equipment uncertainties. To determine the overall uncertainty of experiments, the formula in Equation 1 was employed.

Table 4: Gas analyzer specifications.

Equipment	Method	Measurement	Measurement range	Resolution
BOSCH BEA 350	Infrared pulsating-light	HC	0-9999 ppm	1 ppm
		CO	0-10 % vol.	0.001 % vol.
		CO_2	0-18 % vol.	0.01 % vol.

Overall uncertainty $= \sqrt{}$ (Uncertainity % of ($BSFC^2 + BTE^2 + BP^2 + CO^2 + CO_2^2 + HC^2$)) (1)
$= \sqrt{}$ ($1.3^2 + 0.3^2 + 0.7^2 + 1^2 + 1^2 + 1^2$)
$= \pm$ 2.23%

2.5.2. HFFR test rig

The fuel samples were determined using a DUCOM HFFR kit (Model: TR-281-M8), as shown in Fig. 4. Several specimens were cut into 15 mm × 15 mm test sample plates and polished with silicon carbide sheets of 600, 800, 1000, 1500, and 2000 grit using a polishing machine. The specimens were polished with a-1 and 3 m diamond suspension as an extra layer of polish. After that, a profilometer (Veeco Dektak 150) was used to measure the surface roughness, which was kept between 0.03 and 0.04 (Ra) on the scale. A ball plate was employed on a test sample to study the tribological behavior of fuel samples, in which the steel ball was permitted to glide in a reciprocating motion on a steel specimen, immersed in 5.0 ± 0.2 ml fuel sample. The operating parameters for the tribology test are given in Table 5 and are based on the ASTM D6079-11 standard test procedure. These approaches were developed from the study by Mujtaba et al. (2020b).

After conducting tribological tests, the WSD of the worn steel ball and steel plate was measured using optical microscope (OM). Equation 2 and Equation 3 were applied to calculate the WSD of worn surfaces and the COF, respectively.

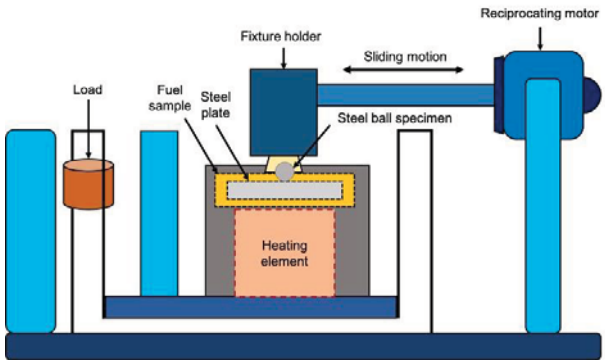

Fig.4 Schematic view of HFRR test rig.

$$WSD = (M + N)/2 \quad (2)$$

in which,
M = major axis (μm) measured through OM
N = minor axis (μm) measured through OM

$$COF = (\text{Actual frictional force (N)})/(\text{Applied Load (N)}) \quad (3)$$

Table 5: HFRR tribological test operating conditions.

Test parameters	Standard value
Sample temperature	60°C
Sample test duration	75 min
Applied load	5 N
Frequency	10 Hz
Stroke length	2 mm
Sample volume	10 ml

2.5.3. Four-ball tribo tester rig

A four-ball tribo tester (FBT-3, Ducom Instruments, Bengaluru, India) was utilized to study the relationship between different fuels and their effect on the tribological characteristics of lubricant, as shown in Fig.5. A temperature sensor was linked to the cup holder, which held three stationary steel balls, and 10 mL of the lubricant sample was added. Four fresh separated steel balls were utilized in each trial. All the tests in this study were done using the standard test method ASTM D4172, and the working conditions in this study are detailed in Table 6. The WSD of the steel ball was measured using OM immediately following the tribological trials. Equation 2 and Equation 3 were used to calculate the WSD of worn surfaces and the COF (Mujtaba et al., 2020b).

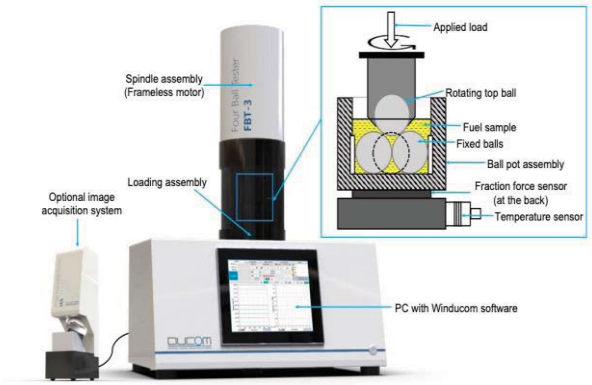

Fig.5 Schematic view of four-ball test rig.

Table 6 Four-ball tribological test operating conditions.

Test parameters	Standard value
Test duration	60 min
Applied load	40 kg
Oil temperature	75 °C
Rotational speed of spindle	1200 rpm

3. RESULTS AND DISCUSSION

3.1. INFLUENCE OF REACTION PARAMETERS ON YIELD OF LIQUID OIL

Experiments were carried out at four different temperatures (300, 350, 400, and 450°C) to see how temperature affected the quality and quality of the liquid oil. Experiments were carried out at three different reaction durations (15, 30, and 45 min) after identifying the ideal temperature to examine the influence on the breakdown of raw materials and liquid oil. The aim of experimenting with various temperatures and reaction periods is to determine the optimal temperature and reaction time for polystyrene waste pyrolysis. The objective of doing the experiment with a 15-minute response time is to examine the decomposition rate at a shorter reaction time to lower the process's excessive energy consumption. The purpose of the 45-minute experiment is to fully breakdown the raw materials and determine the impact of a longer reaction time on the composition and quality of liquid oil and coke production. Fig. 6 depicts the impact of reaction temperature and duration on the yield of WPPO, char, and gas products.

3.1.1. Temperature

Temperature regulates the breaking response of the polymeric chain of polystyrene, making it the most essential process parameter in pyrolysis. Among the many polymers, polystyrene degrades at the lowest temperature (after polyvinyl chloride) in the pyrolysis. Park et al. (2020) investigated the pyrolysis of PS via a continuous two-stage process and found that the main degradation of PS occurred between 300 and 500°C. Fig. 6(a) shows that changing the temperature during a 30-min reaction in a batch pyrolysis reactor resulted in various liquid oil yields. The char production was the highest (6.52 ± 0.25%) at a lower temperature (300 °C), followed by gases (17.83 ± 1.44%) and liquid oil (75.92 ± 1.21%). While the gases output (value) and char yield (value) were the lowest at higher temperatures (400°C). At 400°C, the highest liquid oil production (92.94 ± 2.50%) was reached. Onwudili et al. (2009) also reported maximum liquid oil production around 400°C. At an optimal temperature of 425°C, they found that pyrolysis of polystyrene produced around 97.0 wt.% liquid oil and a maximum gas output of 2.5 wt.%. The additional reaction temperature yields oil and char at a comparable rate as the 400°C reaction temperature. Demirbas (2004) also stated that when pyrolysis was carried out in a batch reactor at 581°C, liquid oil output fell to 89.5 wt.%. As a result, this study did not suggest the pyrolysis of PS at temperatures higher than 500 °C in order to obtain maximal liquid oil output. It is notable that the best reaction temperature in the current study is 400°C and the temperature range for PS degradation during pyrolysis is roughly 300-450°C. Fig. 6 depicts the impact of reaction temperature and duration on the yield of plastic pyrolytic oil, char, and gas products.

3.1.2. Reaction time

The influence of reaction time on liquid oil yield was investigated at 15, 30, and 45 min at the optimal temperature of 400°C. Fig.6(b) indicates that there is a substantial difference in liquid oil production between 15- and 30-min response durations, but no difference between 30- and 45-min reaction times. The maximum liquid oil output was 92.94 ± 2.50% after a 30-min reaction time, compared to 91.38 ± 1.15% after a 45-min reaction time. The char yield was greater when the reaction time was 45 min rather than 30 min (1.14 ± 0.11% versus 1.00 ± 0.001%). The additional reaction time yields a comparable amount of oil and char as the 45-minute reaction time. As a result, 30 min was indicated as the ideal reaction time. The shortest reaction time (15 min) resulted in more char and less liquid oil, suggesting that 15 min was inadequate to convert the feedstock to liquid oil at optimum efficiency. In this investigation, the temperature reaction time for generating maximum liquid oil was observed to be lower than Miandad et al. (2016) (75 min). It is because the influence of reaction time on pyrolysis is dependent on the reactor dimensions and the heat transmission rate from the heating sources to the polystyrene feedstock within the reactor (Ahamed Kameel et al., 2022).

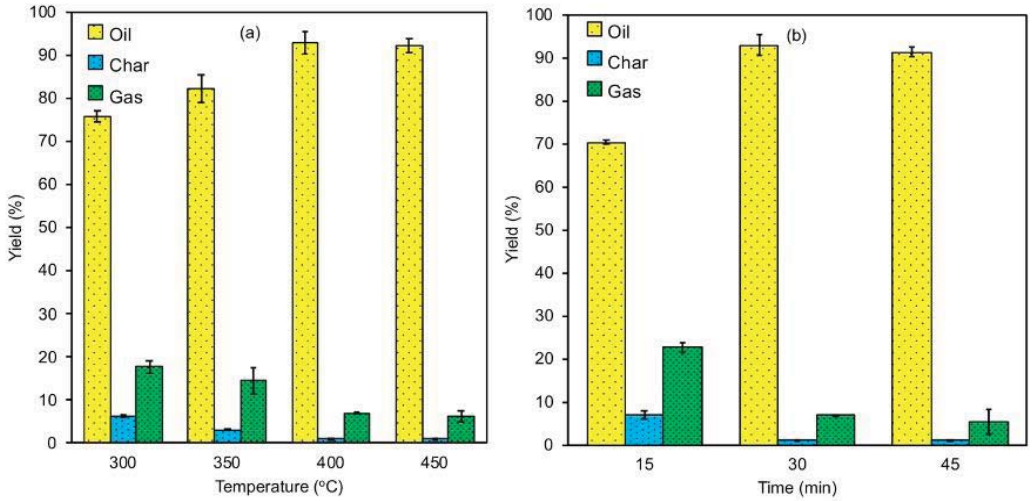

Fig.6 The influence of (a) reaction temperature at a reaction time of 30 min and (b) reaction time at a temperature of 400°C on the yield of plastic pyrolytic oil, char and gas products.

3.2. INFLUENCE OF REACTION PARAMETERS ON PROPERTIES OF LIQUID OIL

Fig.7 depicts the impact of reaction temperature and duration on the properties of PWPO, char, and gas products. High viscosity oil atomizes poorly in the engine oil, resulting in poor engine performance (Miandad et al., 2016). At temperatures of 300, 350, 400, and 450°C, the kinematic viscosity of liquid oil was determined to be 1.29 ± 0.2, 1.44 ± 0.002, 1.33 ± 0.05 and 1.32 ± 0.03 mm^2/s, respectively (Fig.7(a)). Onwudili et al. (2009) found that raising the temperature to 350°C pyrolyzed the whole polystyrene into a dark-coloured liquid oil with a greater viscosity. Longer reaction times diminish kinetic viscosity, as seen in Fig.7(b). A similar tendency was found by Miandad et al. (2016). Due to the presence of a large percentage of gasoline and a low fraction of heavy oil, the liquid oil generated in this investigation had a lower kinematic viscosity than diesel fuel (Table 1) (Syamsiro et al., 2014). Kinematic viscosity is also important in engine lubrication, particularly for rotary distributor injection pump (Hansen, Zhang, & Lyne, 2005). Low kinematic viscosity fuel can cause injector leaks, leading to poor engine performance (Syamsiro et al., 2014).

Any petroleum product's density is a critical metric. At temperatures of 300, 350, 400, and 450°C, the generated liquid oils had densities of 0.952 ± 0.008, 0.958 ± 0.002, 0.955 ± 0.002 and 0.956 ± 0.0003 g/cm^3, respectively (Fig.7(a)). This density range is consistent with the previously reported pyrolysis liquid oil density ranges using the same feedstock (Miandad et al., 2016). The reaction temperature does not appear to impact the density. As illustrated in Fig.7(b), the similar pattern can be found in reaction time. The findings are consistent with those of Miandad et al. (2016). Furthermore, this density range is somewhat greater than commercial diesel (Table 1). One of the most significant properties of fuels is their calorific value. According to Saptoadi and Pratama (2015), greater calorific value fuels require fewer calories to accomplish the same function as lower calorific value fuels. At 300, 350, 400, and 450°C, the liquid oil generated from polystyrene plastic exhibited calorific values of 39.11± 1.73, 40.98 ± 1.63, 39.94 ± 0.43, ± 40.61 ± 0.25 MJ/kg, respectively (Fig.7(a)). According to Miandad et al. (2016), increasing the temperature (from 400 to 500°C) increased the calorific value of liquid oil (from 37.48 to 41.58 MJ/kg), which is consistent with our findings. Furthermore, the generated liquid oil had a somewhat lower calorific value (46.57 MJ/kg) than traditional diesel (Table 1). Table 7 shows that the properties of the liquid oil generated in this investigation are equivalent to those of earlier experiments.

3.3. GC-MS ANALYSIS

The carbon number range of alkane and alkene, as well as the composition of aromatic products of B10 and PS100, are shown in Fig.8**.** GC-MS data of B10 portrays that the majority of its chemical components is alkanes. Alkanes, benzene, naphthalene, and alkenes are 50.7, 4.9, 4.0, and 0.3% of B10, respectively. Mangesh et al. (2020) found the same quantity of alkanes, as well as the same benzene (28.8%) and naphthalene concentration (13.7%). PS100 has 34.6% aromatics, 25.2% alkanes, and 4.3% alkenes, according to GC-MS findings. PS100 has a 43.7%

greater olefin content than B10. The same tendency was noticed by Mangesh et al. (2020). The unsaturated double bonds in olefin compounds emit a lot of heat during the diesel engine combustion (Mangesh et al., 2020).

Fig.8(a) shows that the GC-MS data was sorted by the number of carbon atoms in the alkane compounds found in B10 and PS100. The C_{13}-C_{17}, C_{18}-C_{22} and C_8-C_{12} ranges, respectively, account for 32,7, 11.5, and 4.2% of the B10. PS100 has the majority of alkanes in the C_{13}-C_{17} range, however they are 64.7% less than B10. PS100 has a lower alkene concentration in the C_{18}-C_{22} and C_8-C_{12} ranges than B10, by 98.2 and 68.2%, respectively. The viscosity of PS100 is lower than that of B10, as indicated in Table 1. This is due to the lower concentration of alkanes in PO100 than in B10. Fig.8(a) further reveals that alkanes in the C_{23}-C_{27} and C_{28}-C_{32} ranges are exclusively found in PS100.

The GC-MS data was sorted based on the carbon number range of the olefin compounds found in B10 and PS100, as shown in Fig.8(b). PS100 has a 43.74% greater olefin content than B10 in the C_8-C_{12} carbon number range (gasoline fraction content). Fig.8(b) further demonstrates that alkanes with higher carbon numbers (C_{13}-C_{17} and C_{18}-C_{22}) are exclusively found in PS100. When comparing PS100 to B10, the presence of greater carbon number compounds results in increased CO and CO_2 emissions. PWPO, on the other hand, is thought to have a low concentration of heavy HC (C_{20} and above, around 6%). Similar results were also obtained by Singh et al. (2020). The GC-MS results for aromatic compounds found in B10 and PO100 are shown in Fig.8(c). PO100 contains 34.6% aromatic compounds, which is somewhat less than the previous studies' estimation of 39% (Damodharan et al., 2017). PO100 has a greater benzene and naphthalene concentration than B10, with 123.5% and 109.3%, respectively.

Table 7: Comparison of properties of PWPO with previous studies.

Reference	Current study	Miandad et al. (2016)	Kalargaris et al. (2017b)	Khan et al. (2016)	Kalargaris et al. (2018)	Kumar et al. (2020)
Type of plastic	PS	PS	LDPE	HDPE	PP	PET
Density (g/cm^3)	0.9388	0.92	0.84	0.75	0.84	0.75
Kinematic viscosity (mm^2/s)	1.4302	1.92	3.00	1.98	1.50	1.55
Calorific value (MJ.kg)	43.508	41.6	42.4	41.13	40.80	NR

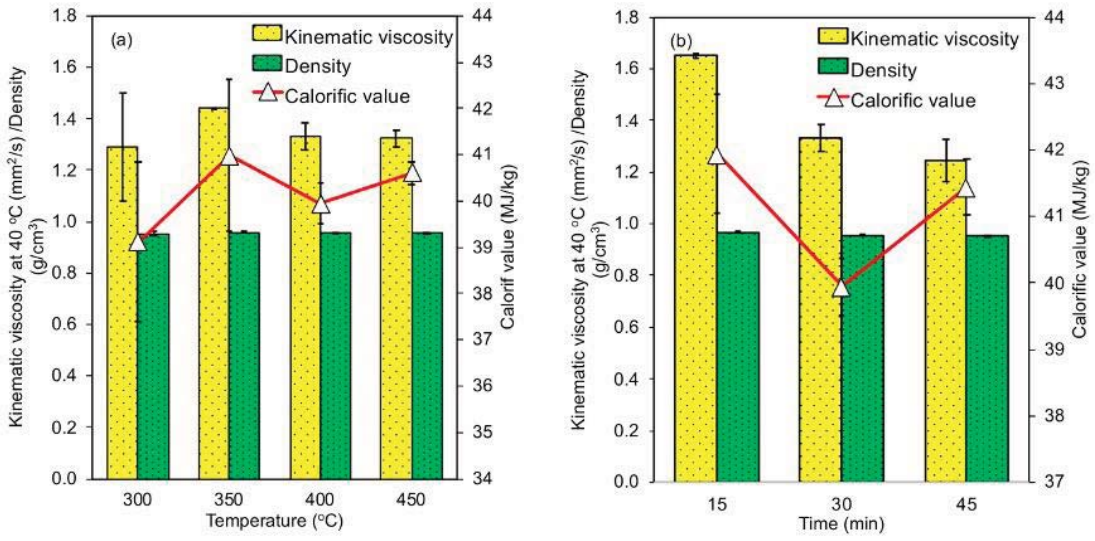

Fig.7 The influence of (a) reaction temperature at a reaction time of 30 min and (b) reaction time at a temperature of 400 °C on the properties of plastic pyrolytic oil products.

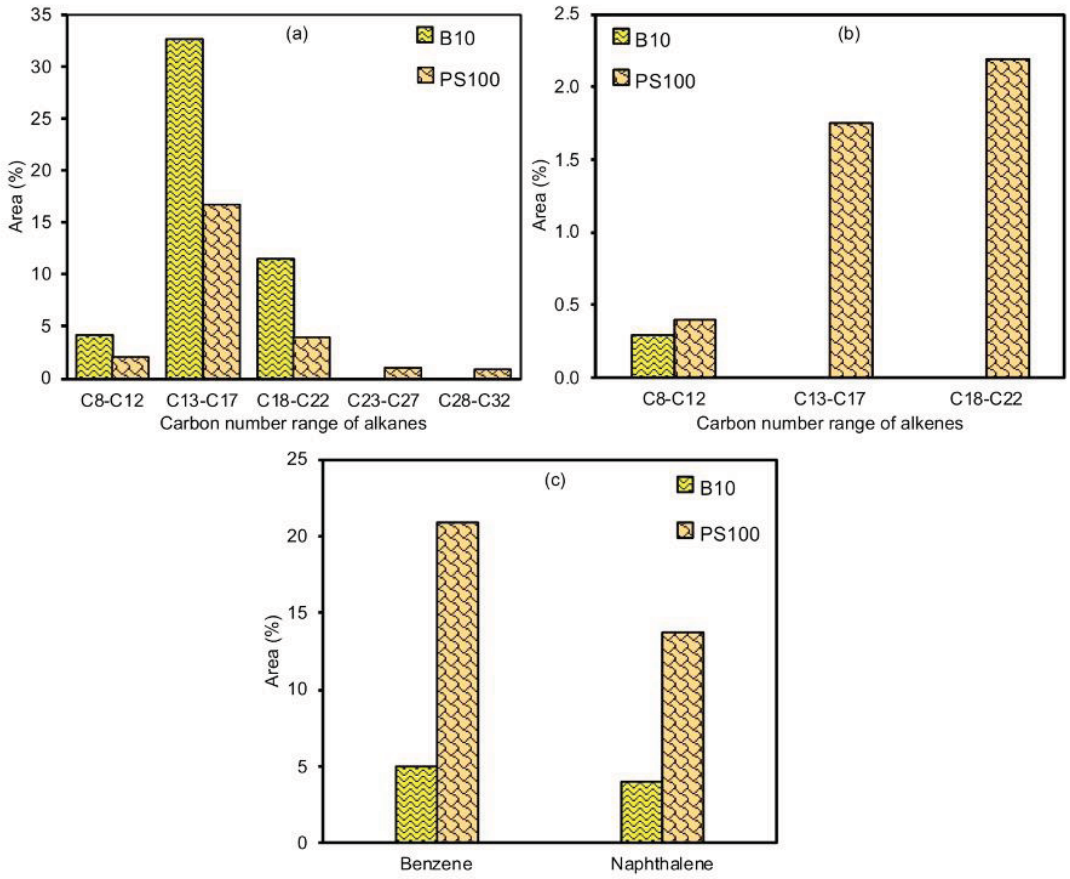

Fig.8 Carbon number range of (a) alkane and (b) alkene products, and (c) composition of aromatic products of B10 and PS100.

3.4. ENGINE PERFORMANCE

3.4.1. Brake thermal efficiency

At full engine load, Fig.9(a) depicts the BTE changes for B10 and PS100 (900 to 2400 rpm). Due to a poor air-fuel mixing and spray characteristics at higher speeds, all fuel samples indicate a BTE rise at 2100 rpm and subsequently a minor reduction at 2400 rpm. At 2100 rpm, the highest BTE values for B10 and PS100 were 25.4 and 21.7%, respectively. At all engine speeds, the average BTE values of PS100 and B10 were 21.8 and 18.7%, respectively. PS100 had a 15.5% greater BTE than B10, owing to its reduced viscosity, which outweighed its lower calorific value, resulting in superior atomization and combustion efficiency (Awang et al., 2021). The findings contradict those of Kalargaris et al. (2017a) who found that pyrolytic oil from mixed plastic trash had a lower BTE of 9.3% than diesel. Thus, mixing PS100 with B10 can enhance mixed fuel BTE.

3.4.2. Brake-specific fuel consumption

Fig.9(b) shows the BSFC values for B10 and PS100 fuels while the engine is running at full load with a changing engine speed. The BSFC of all fuel samples declined as engine speed increased to 2100 rpm, then reduced marginally at 2400 rpm. At 2100 rpm, the lowest BSFC values for all tested fuels (PS100 and B10) were 0.32 and 0.36 kg/kWh, respectively. PS100 and B10 have average BSFCs of 0.39 and 0.42 kg/kWh, respectively. PS100 had an average BSFC that was 8.0% lower than B10. Its reduced viscosity, which outweighs its lower calorific value and higher density, results in a superior air-fuel combination and atomization effect. The effort required during the compression stroke is reduced as volumetric efficiency improves, increasing the BSFC value of PS100 (Khalife et al., 2017; Murcak et al., 2013). The findings contrast those of Kalargaris et al. (2017a), who found that pyrolytic oil made from mixed plastic waste had a 25.5% lower BSCF than diesel. The results, however, are equivalent to those obtained in experiments using oxygen-containing alcohol fuel additives (Prabu et al., 2018; Sharonet al., 2013). Furthermore, WPPO's high volatility can contribute to a better air-fuel combination, resulting in a better combustion process and higher combustion efficiency (Chandran, Senthilkumar, & Murugesan, 2019; Khan et al., 2016; Mujtaba, et al., 2020c). Due to the rapid evaporation rate, the quaternary

fuel's small fuel droplets increase air-fuel mixing and hence improve combustion characteristics.

3.4.3. Engine brake power

Fig.9(c) depicts the engine BP of the B10 and PS100 engines as a function of engine speed under 100% load. At all speeds, there was a substantial difference in the BP of each fuel. It is evidenced that the BP of all samples is increasing as the speed increases. The highest BP values found at 2400 rpm for PS100 and B10 are 7.8 and 7.2 kW, respectively. PS100 and B10 have average BPs of 5.6 and 5.3 kW, respectively. PS100 has a 5.6% higher average blood pressure than B10. When compared to B10, PS100's lower viscosity might result in power loss due to the greater fuel pump leakages (Liu, Tan, & Cao, 2020).

3.4.4. Engine brake torque

Fig.9(d) depicts the BT for all fuel samples at 100% engine load with varying engine speed. At low speeds, all of the fuels tested showed a rise in BT value, followed by a reduction at middle speeds. The average BT value of all tested fuels declined as the speed climbed from 1500 to 2400 rpm. This is because the combustion chamber was not sufficiently filled during the intake stroke, and the valve's volumetric efficiency was declined as a result of the complete opening of the valve because there was inadequate time for a sufficient intake phase, resulting in a decrease in combustion chamber pressure (Aguerre et al., 2022). At 1800 rpm, the highest torque values for PS100 and B10 were 34.0 and 32.3 Nm, respectively. PS100 and B10 had average BTs of 32.61 and 31.1 Nm, respectively. In comparison to B10, PS100 had a 2.4% higher average BTE value.

3.5. EXHAUST ENGINE EMISSIONS

3.5.1. Hydrocarbon emission

Fig.10(a) depicts the changes in HC emissions for the B10 and PS100 engines as a function of speed. With rising speed, HC emissions from all fuels dropped. At a speed of 900 rpm, the maximum HC emissions of all fuel samples were measured. In comparison to the low engine speed, all fuels had decreased HC emissions when the engine speed was at its maximum. The same tendency was observed by Awang et al. (2021). B10 and PS100 had average HC emissions of 5.7 and 11.17 ppm vol, respectively. PS100's HC emissions are 97.06% greater than B10's due to their low volatility (Nabi et al., 2015). In comparison to diesel, Kalargaris et al. (2017a) discovered that PPO produced 97.1% more HC emissions. PS100 also contains more aromatics (117.7% more aromatics than B10), which reduces the burning period and increases the ignition delay time, resulting in higher HC emissions. This is also owing to its high density, which outweighs its low viscosity, resulting in big droplet formation, inadequate fuel-air mixing, and low vapour pressure, leading in incomplete combustion and higher HC emissions (Nabi et al., 2015; Singh et al., 2020). This can be because B10 has a greater oxygen concentration than PS100, resulting in more efficient combustion (Awang et al., 2021). The tendency is consistent with previous research (Kalargaris et al., 2017a; Kumar et al., 2016), although with a considerably lower increase (approximately 43.8 to 85.1%).

3.5.2. Carbon monoxide emission

Fig.10(b) depicts the impact of CO emissions on speed for the fuels that were evaluated. At 900 rpm, the highest CO emissions of all fuel samples were measured. With increased speed, CO emissions drop. The rate at which CO is converted to CO_2 rises at higher engine speeds, as illustrated in Fig. 10(b), because the high air-fuel ratio and temperature, decreasing CO emissions. Because of their lower calorific value, PS100 emitted 702.0% more CO than B10, respectively. This results in a greater amount of fuel injection for the same load situation, resulting in a greater amount of CO emission (Kalargaris et al., 2017a). PS100 emitted more CO than B10 because its higher density outweighed its lower viscosity, resulting in poor air-fuel mixing, mainly at low speeds. As a result of insufficient fuel–air mixing, which causes incomplete combustion, CO emissions rise (Ruhul et al., 2016). This pattern is consistent with earlier research, which found that WPPO emits 33.9-102.2% more CO than diesel (Kalargaris et al., 2017a; Kumar et al., 2016).

3.5.3. Carbon dioxide emission

A complete combustion occurs when all the carbon atoms in the fuel are completely oxidized, resulting in CO_2 emissions. It is not subjected to emission regulations and is not classified as a hazardous gas. However, because CO_2 is a greenhouse gas, it is critical to limit CO_2 emissions (Kalargaris et al., 2017a; Singh et al., 2020). The CO_2 emissions of B10 and PS100 are shown in Fig.10(c). B10 and PS100 had average CO_2 emissions of 7.4 and 8.6 %vol, respectively. When compared to B10, the CO_2 emissions of PS100 are 17.2% on average. This is due to the existence of larger carbon number compounds in PS100 diesel compared to B10 diesel, as illustrated in Fig.8 (Mangesh et al., 2020; Nabi et al., 2015). This finding is in line with the findings of earlier research, which found that PPO emits more CO_2 than diesel (Kalargaris et al., 2017a; Mangesh et al., 2020; Singh et al., 2021).

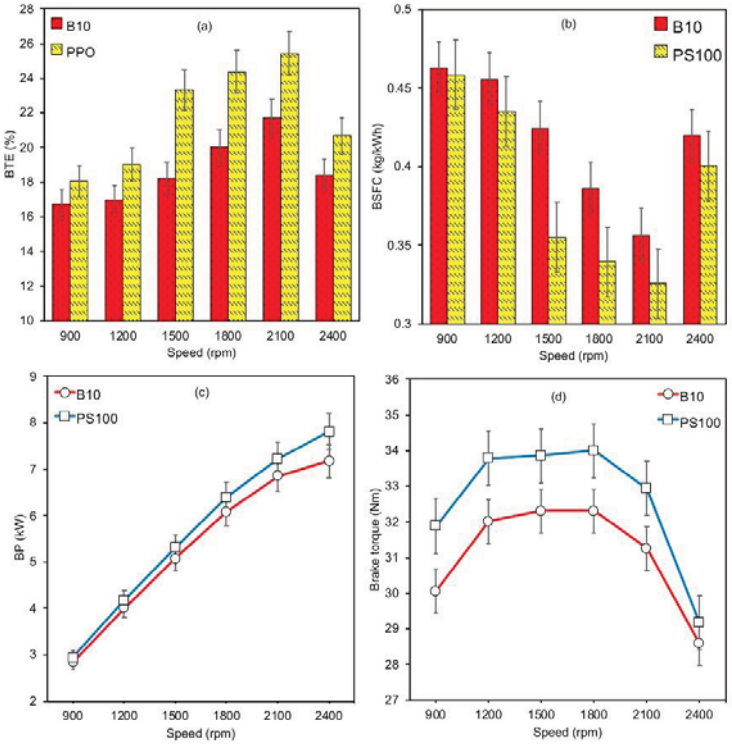

Fig.9(a) Variation of BTE, (b) BSFC, (c) BP and (d) BT for B10 and PS100 according to engine speed at full load condition.

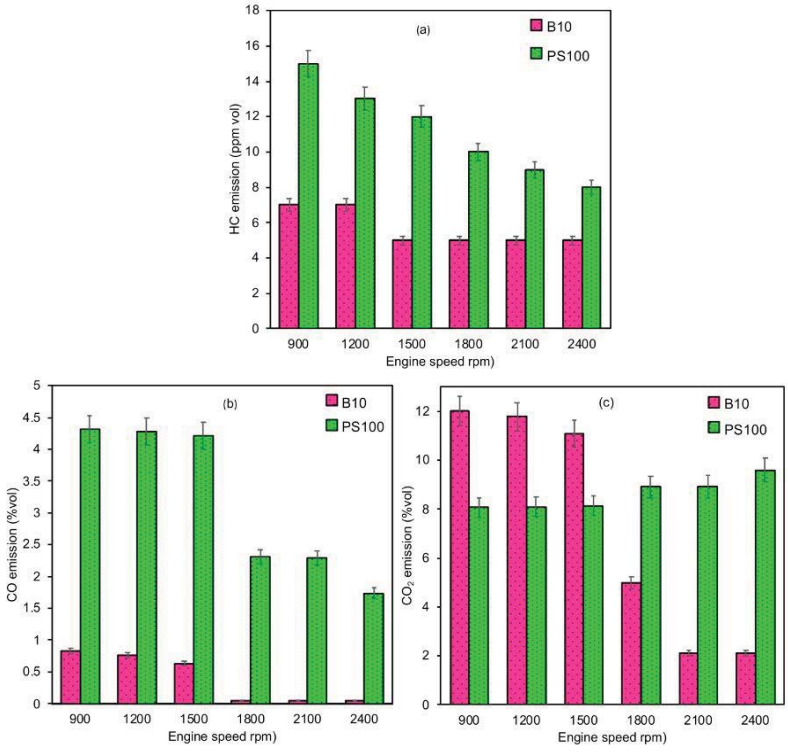

Fig.10(a) Variation of (a) HC, (b) CO and (c) CO_2 emissions for all tested fuels according to engine speed at full load condition.

3.6. HFRR TRIBOLOGICAL STUDY

Fig.11(a) depicts the COF pattern of all HFRR fuel samples throughout time. Due to no lubricating coating between the contact surfaces in the early phases of the experiment, the COF of all samples was high. It is known as the running-in period. Between the contact surfaces, a lubricating layer develops, and the surface roughness between the friction surfaces smooths out over time. The steady state refers to this stage of the experiment (Awang et al., 2022). The B10 fuel sample had the shortest run-in time. The average COF and WSD values of all fuel samples are shown in Fig.11(b). B10 and PS100 had average COF values of 0.073 and 0.086, respectively. B10 and PS100 have WSDs of 1.20 and 1.36 mm, respectively. PS100 had a COF and WSD that were 27.6% and 12.3% greater than B10, respectively. PS100's low viscosity causes a thinner and weaker lubricating layer between mating balls, resulting in a rise in average COF (Awang et al., 2020). This finding is in line with that of Awang et al. (2020), who found that pyrolytic oil from low-density polyethylene had a 4.2 and 13.2% higher COF and WSD value, respectively.

3.7. FOUR-BALL TRIBOLOGICAL STUDY

Fig.12 depicts the impact of B10 and PS100 on mineral lubricant lubricity. According to earlier research, the lubricant could be up to 5% contaminated with fuel owing to crankcase thinning (Awang et al., 2022). The lubricant had been contaminated with combustible fuel, which changed the lubricant's tribological characteristics and led to poor lubricating properties owing to lubricant deterioration. The COF patterns for all examined samples are shown in Fig.12(a). Because of its superior lubricating qualities, the running-in period of pure mineral lubricant was considerably reduced. The steady-state conditions were rapidly reached due to the development of a lubricating layer between the metallic contacts during the early part of the test run (Awang et al., 2022). When compared to other lubricant-contaminated samples, the mineral lubricant had a considerably lower COF (0.11). The lubricant's lubricating characteristics were changed when combustible fuel was added, leading to poor tribological performance. Fig.12(a) further shows that as compared to B10, the mineral lubricant contaminated with blank PS100 showed higher lubricant degradation. Because of the reduced viscosity, the average COF for SAE40-PS100 was 29.8% greater than for SAE40-B10. This had a significant influence on the fuel lubricity. Different trends can be observed in the value of WSD. SAE40-PS100 had a WSD that was 12.6% higher than SAE40-B10.

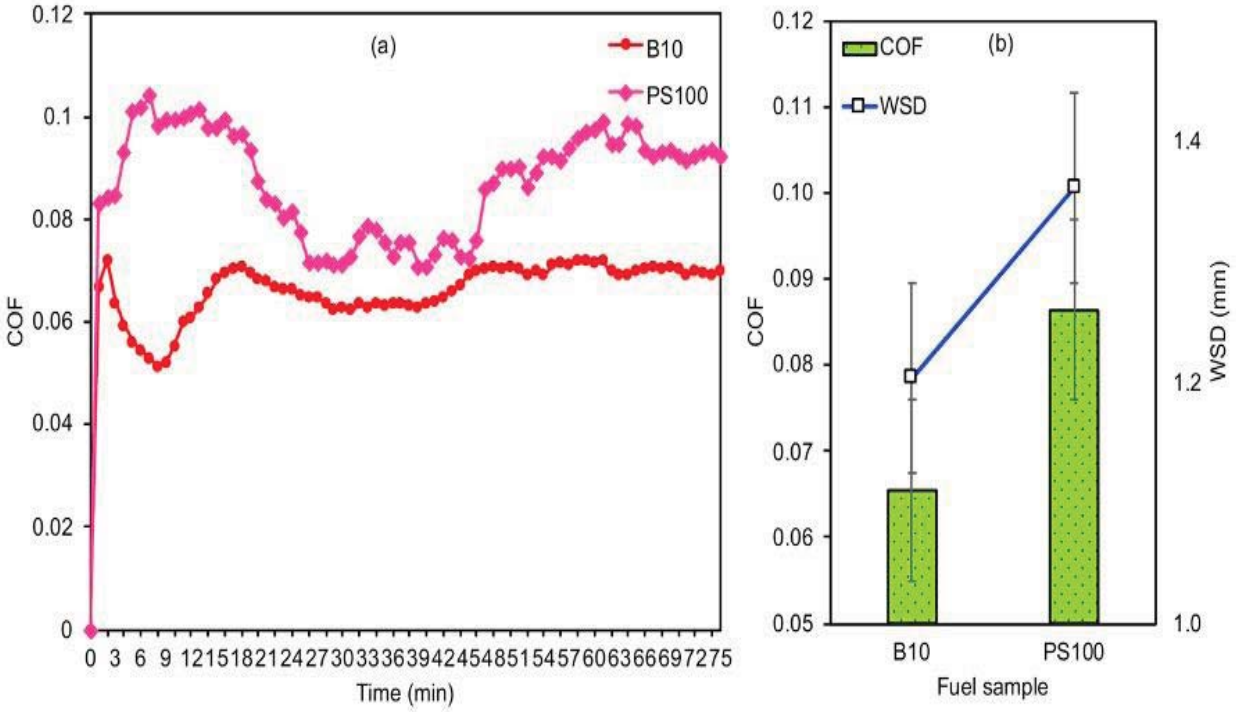

Fig.11(a) COF during the run-in period and steady-state period and (b) average COF and WSD.

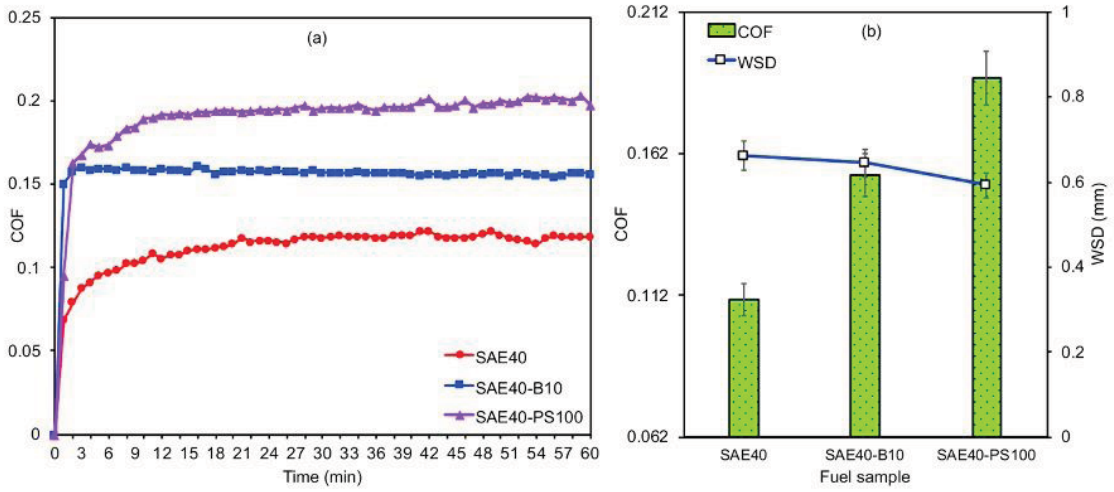

Fig.12(a) COF during the run-in period and steady-state period and (b) average COF and WSD for mineral lubricant and lubricant contaminated samples.

3.8. Limitations of PWPO

The average parameter changes for PS100 fuel compared to B10 diesel are summarized in Fig.13. In terms of performance, PS100 outperformed B10, with higher BTE, BP, and BT by 15.5, 5.6, and 2.38 %, respectively, but a lower BSFC of 8.0%. PS100, on the other hand, emitted 97.06, 702.0, and 17.3% more HC, CO, and CO2 than B10. Its poor exhaust gas emissions have proven as a key stumbling block in its application in diesel engines. Mujtaba et al. (2020) recommended the application of oxygenated alcohols like dimethyl carbonate (DMC) and diethyl ether (DEE) in fuel samples to enhance engine emission characteristics. PS100 also demonstrated a 27.6% increase in COF and a 29.8% increase in lubricant contamination as compared to B10 diesel. When nanoparticles are added to fuel mixes, the lubricity and tribological characteristics increase, leading to a reduced COF when compared to fuel samples without nanoparticles (Mujtaba et al., 2020b; Razzaq et al., 2021). This is due to the nanoparticles act as a sacrificial layer between the friction surfaces. Due to the presence of nanoparticles between the metallic contacts, Razzaq et al. (2021) found that graphene oxide nanoplatelets in diesel-biodiesel-alcohol fuel mixes had a reduced COF. Mujtaba et al. (2020b), who employed titanium oxide nanoparticles in palm-sesame methyl ester-diesel mixtures, obtained the same observation.

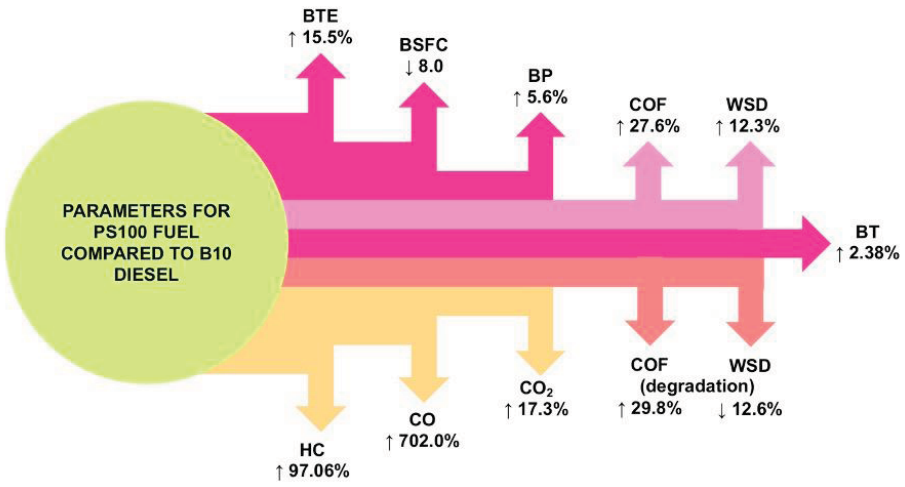

Fig.13 Average percent change in the parameters measured for PS100 fuel compared with B10 diesel fuel.

4. CONCLUSION

A small-scale batch reactor was utilized to pyrolyze the polystyrene plastic waste to liquid oil in this work. The impact of temperature and reaction time on liquid oil quality and yield was also discussed in this work. The findings revealed that at lower temperature (300 °C), liquid oil output was low while char yield was very significant. The ideal temperature and reaction time were discovered to be 400 °C and 30 min, respectively and the produced liquid oil at these ideal conditions has a density of 0.94 kg/m^3, a kinematic viscosity of 1.43 mm^2/s, and a calorific value of 43.51 MJ/kg. The properties are comparable to the value of B10 commercial diesel. PS100 includes 34.6% aromatics, 25.2% alkanes, and 4.3% alkenes, according to GC-MS analysis.

Following that, the optimally produced liquid oil was tested as a fuel in a diesel engine to see how it performed. In terms of performance, PS100 beat B10, with higher BTE, BP, and BT by 15.5, 5.6, and 2.38 %, respectively, but a lower BSFC of 8.0%. PS100, on the other hand, emitted 97.06, 702.0, and 17.3% more HC, CO, and CO_2 than B10. Its poor exhaust gas emissions have proven a key stumbling block in its application in diesel engines. PS100 also demonstrated a 27.6% increase in COF and a 29.8% increase in lubricant contamination as compared to B10 diesel.

For diesel engine applications, oxygen-enriched alcohols (such as DMC and DEE) and nanoparticles (such as graphene oxide nanoplatelets and titanium oxide nanoparticles) will be added to the PS100 in the future. PS100 fuel with additive will enhance fuel properties, as well as engine emission and performance metrics, as well as wear characteristics. Due to the growing need for alternative fuels, PWPO will soon become a viable option to the next generation of fuels. PWPO can also be mixed with commercial diesel to improve certain fuel properties and, as a result, diesel engine performance, without requiring the diesel engine to be modified.

ACKNOWLEDGEMENTS

The authors take the opportunity to thank Universiti Malaya for the financial support under research grant IIRG008B-2019 under Universiti Malaya Impact-Oriented Interdisciplinary Research Grant Programme.

REFERENCES

Aguerre, H.J., Pedreira, P.H., Orbaiz, P.J., and Nigro, N.M. 2022. Validation and Enhancement of a Supermesh Strategy for the CFD Simulation of Four-Stroke Internal Combustion Engines, Fluids 7(3): 104.

Ahamed Kameel, N.I., Wan Daud, W.M.A., Abdul Patah, M.F., and Mohd Zulkifli, N.W. 2022. Influence of reaction parameters on thermal liquefaction of plastic wastes into oil: A review, Energy Conversion and Management: X 14: 100196.

Awang, M.S., Zulkifli, N.W., Abbas, M.M., Zulkifli, S.A., Yusoff, M.N., Ahmad, M.H., Lokman NolHakim, M.A. and Wan Daud, W.M. 2021. Effect of addition of plastic pyrolytic oil and waste cooking oil biodiesel in palm oil biodiesel–commercial diesel blends on diesel engine performance, emission, and lubricity, Energy & Environment 0958305X211034822.

Awang, M.S.N., Mohd Zulkifli, N.W., Abbas, M.M., Amzar Zulkifli, S., Kalam, M.A., Ahmad, M.H., Mohd Yusoff, M.N.A., Mazlan, M. and Daud, W.M.A.W. 2021. Effect of addition of palm oil biodiesel in waste plastic oil on diesel engine performance, emission, and lubricity, ACS omega 6(33): 21655-21675.

Awang, M.S.N., Zulkifli, N.W.M., Abbas, M.M., Zulkifli, M.S.A., Kalam, M.A., Yusoff, M.N.A.M., Ahmad, M.H. and Daud, W.M.A.W. 2022. Effect of plastic pyrolytic oil and waste cooking biodiesel on tribological properties of palm biodiesel–diesel fuel blends, Industrial Lubrication and Tribology.

Awang, M.S.N., Zulkifli, N.W.M., Abbas, M.M., Zulkifli, S.A., Kalam, M.A., Yusoff, M.N.A.M., Daud, W.M.A.W. and Ahmad, M.H. 2022. Effect of diesel-palm biodiesel fuel with plastic pyrolysis oil and waste cooking biodiesel on tribological characteristics of lubricating oil, Alexandria Engineering Journal 61(9): 7221-7231.

Awang, M.S.N., Zulkifli, N.W.M., Abbass, M.M., Zulkifli, S.A., Yusoff, M.N.A.M., Ahmad, M.H. and Daud, W.M.A.W. 2020. Effect of blending local plastic pyrolytic oil with diesel fuel on lubricity, Jurnal Tribologi 27: 143-157.

Chandran, M., Tamilkolundu, S. and Murugesan, C. 2020. Characterization studies: waste plastic oil and its blends, Energy Sources, Part A: Recovery, Utilization, and Environmental Effects 42 (3): 281-291.

Damodharan, D., Sathiyagnanam, A.P., Rana, D., Kumar, B.R. and Saravanan, S. 2017. Extraction and characterization of waste plastic oil (WPO) with the effect of n-butanol addition on the performance and emissions of a DI diesel engine fueled with WPO/diesel blends, Energy conversion and management 131: 117-126.

Demirbas, A. 2004. Pyrolysis of municipal plastic wastes for recovery of gasoline-range hydrocarbons, Journal of Analytical and Applied Pyrolysis 72 (1): 97-102.

Gul, M., Masjuki, H.H., Kalam, M.A., Zulkifli, N.W.M. and Mujtaba, M.A. 2020. A review: role of fatty acids composition in characterizing potential feedstock for sustainable green lubricants by advance transesterification process and its global

as well as Pakistani prospective, BioEnergy Research 13 (1): 1-22.
Hansen, A.C., Zhang, Q. and Lyne, P.W. 2005. Ethanol–diesel fuel blends—a review, Bioresource technology 96 (3): 277-285.
Juwono, H., Fauziah, L., Uyun, I.Q., Alfian, R., Suprapto, Ni'mah, Y.L. and Ulfin, I. 2018. Catalytic convertion of Al-MCM-41-ceramic on ydrocarbon (C8–C12) liquid fuel synthesis from polypropylene plastic waste, AIP conference proceedings 2049 (1): 020080.
Kaewbuddee, C., Sukjit, E., Srisertpol, J., Maithomklang, S., Wathakit, K., Klinkaew, N., Liplap, P. and Arjharn, W. 2020. Evaluation of waste plastic oil-biodiesel blends as alternative fuels for diesel engines, Energies 13 (11): 2823.
Kaimal, V.K. and Vijayabalan, P. 2015. A detailed study of combustion characteristics of a DI diesel engine using waste plastic oil and its blends, Energy conversion and Management 105: 951-956.
Kalargaris, I., Tian, G. and Gu, S. 2017a. Combustion, performance and emission analysis of a DI diesel engine using plastic pyrolysis oil, Fuel Processing Technology 157: 108-115.
Kalargaris, I., Tian, G. and Gu, S. 2017b. Experimental evaluation of a diesel engine fuelled by pyrolysis oils produced from low-density polyethylene and ethylene–vinyl acetate plastics, Fuel Processing Technology 161: 125-131.
Kalargaris, I., Tian, G. and Gu, S. 2018. Experimental characterisation of a diesel engine running on polypropylene oils produced at different pyrolysis temperatures, Fuel 211: 797-803.
Khairil, Kumar, R., Riayatsyah, T.M.I., Jalaluddin and Sofyan, S. 2020. The potential plastic oil production from plastics waste (PET and LDPE) in Aceh, Indonesia, IOP Conference Series: Earth and Environmental Science 505: 012027.
Khalife, E., Tabatabaei, M., Demirbas, A. and Aghbashlo, M. 2017. Impacts of additives on performance and emission characteristics of diesel engines during steady state operation, Progress in energy and Combustion Science 59: 32-78.
Khan, M.Z.H., Sultana, M., Al-Mamun, M.R. and Hasan, M.R. 2016. Pyrolytic waste plastic oil and its diesel blend: fuel characterization, Journal of environmental and public health.
Kin, W.E. and Jasmin, A.F. 2019. Plastic: an undegradable problem, License: Creative Commons Attribution CC BY, 3.
Kumar, R., Mishra, M.K., Singh, S.K. and Kumar, A. 2016. Experimental evaluation of waste plastic oil and its blends on a single cylinder diesel engine, Journal of mechanical science and technology 30 (10): 4781-4789.
Liu, M., Tan, L., & Cao, S. 2020. Influence of viscosity on energy performance and flow field of a multiphase pump, Renewable Energy 162: 1151-1160.
Mangesh, V.L., Padmanabhan, S., Tamizhdurai, P. and Ramesh, A. 2020. Experimental investigation to identify the type of waste plastic pyrolysis oil suitable for conversion to diesel engine fuel, Journal of Cleaner Production 246: 119066.
Mangesh, V.L., Padmanabhan, S., Tamizhdurai, P. and Ramesh, A., 2020. Experimental investigation to identify the type of waste plastic pyrolysis oil suitable for conversion to diesel engine fuel, Journal of Cleaner Production 246: 119066.
Mani, M., Subash, C. and Nagarajan, G. 2009. Performance, emission and combustion characteristics of a DI diesel engine using waste plastic oil, Applied thermal engineering 29 (13): 2738-2744.
Miandad, R., Nizami, A.S., Rehan, M., Barakat, M.A., Khan, M.I., Mustafa, A., Ismail, I.M.I. and Murphy, J.D. 2016. Influence of temperature and reaction time on the conversion of polystyrene waste to pyrolysis liquid oil, Waste Management 58: 250-259.
Mujtaba, M.A., Cho, H.M., Masjuki, H.H., Kalam, M.A., Ong, H.C., Gul, M., Harith, M.H. and Yusoff, M.N.A.M. 2020a. Critical review on sesame seed oil and its methyl ester on cold flow and oxidation stability, Energy Reports 6: 40-54.
Mujtaba, M.A., Kalam, M.A., Masjuki, H.H., Gul, M., Soudagar, M.E.M., Ong, H.C., Ahmed, W., Atabani, A.E., Razzaq, L. and Yusoff, M. 2020c. Comparative study of nanoparticles and alcoholic fuel additives-biodiesel-diesel blend for performance and emission improvements, Fuel 279: 118434.
Mujtaba, M.A., Masjuki, H.H., Kalam, M.A., Noor, F., Farooq, M., Ong, H.C., Gul, M., Soudagar, M.E.M., Bashir, S., Rizwanul Fattah, I.M. and Razzaq, L. 2020b. Effect of additivized biodiesel blends on diesel engine performance, emission, tribological characteristics, and lubricant tribology, Energies 13 (13): 3375.
Murcak, A., Haşimoğlu, C., Çevik, İ., Karabektaş, M. and Ergen, G. 2013. Effects of ethanol–diesel blends to performance of a DI diesel engine for different injection timings, Fuel 109: 582-587.
Nabi, M.N., Rahman, M.M., Islam, M.A., Hossain, F.M., Brooks, P., Rowlands, W.N., Tulloch, J., Ristovski, Z.D. and Brown, R.J. 2015. Fuel characterisation, engine performance, combustion and exhaust emissions with a new renewable Licella biofuel, Energy Conversion and management 96: 588-598.
Onwudili, J.A., Insura, N. and Williams, P.T. 2009. Composition of products from the pyrolysis of polyethylene and polystyrene in a closed batch

reactor: Effects of temperature and residence time, Journal of Analytical and Applied Pyrolysis 86 (2): 293-303.
Park, K.-B., Jeong, Y.-S., Guzelciftci, B., and Kim, J.-S. 2020. Two-stage pyrolysis of polystyrene: Pyrolysis oil as a source of fuels or benzene, toluene, ethylbenzene, and xylenes, Applied Energy 259: 114240.
Razzaq, L., Mujtaba, M.A., Soudagar, M.E.M., Ahmed, W., Fayaz, H., Bashir, S., Fattah, I.R., Ong, H.C., Shahapurkar, K., Afzal, A. and Wageh, S. 2021. Engine performance and emission characteristics of palm biodiesel blends with graphene oxide nanoplatelets and dimethyl carbonate additives, Journal of environmental management, 282: 111917.
Rizwanul Fattah, I.M., Ong, H.C., Mahlia, T.M.I., Mofijur, M., Silitonga, A.S., Rahman, S.M. and Ahmad, A. 2020. State of the art of catalysts for biodiesel production, Frontiers in Energy Research 8: 101.
Ruhul, M.A., Abedin, M.J., Rahman, S.A., Masjuki, B.H.H., Alabdulkarem, A., Kalam, M.A. and Shancita, I. 2016. Impact of fatty acid composition and physicochemical properties of Jatropha and Alexandrian laurel biodiesel blends: An analysis of performance and emission characteristics, Journal of cleaner production 133: 1181-1189.
Sachuthananthan, B., Reddy, D., Mahesh, C. and Dineshwar, B. 2018. Production of diesel like fuel from municipal solid waste plastics for using in CI engine to study the combustion, performance and emission characteristics, International Journal of Mathematics and Mathematical Sciences 119: 85-96.
Saptoadi, H. and Pratama, N.N. 2015. Utilization of plastics waste oil as partial substitute for kerosene in pressurized cookstoves, International Journal of Environmental Science and Development 6 (5): 363.
Senthur Prabu, S., Asokan, M.A., Prathiba, S., Ahmed, S., and Puthean, G. 2018. Effect of additives on performance, combustion and emission behavior of preheated palm oil/diesel blends in DI diesel engine, Renewable Energy 122: 196-205.
Sharon, H., Ram, P.J.S., Fernando, K.J., Murali, S. and Muthusamy, R. 2013. Fueling a stationary direct injection diesel engine with diesel-used palm oil–butanol blends–an experimental study, Energy conversion and management 73: 95-105.
Singh, R., Ruj, B., Sadhukhan, A., and Gupta, P. 2019. Thermal degradation of waste plastics under non-sweeping atmosphere: Part 1: Effect of temperature, product optimization, and degradation mechanism, Journal of environmental management 239: 395-406.
Singh, R.K., Ruj, B., Sadhukhan, A.K., Gupta, P. and Tigga, V.P. 2020. Waste plastic to pyrolytic oil and its utilization in CI engine: Performance analysis and combustion characteristics, Fuel 262: 116539.
Singh, T.S., Rajak, U., Dasore, A., Muthukumar, M. and Verma, T.N. 2021. Performance and ecological parameters of a diesel engine fueled with diesel and plastic pyrolyzed oil (PPO) at variable working parameters, Environmental Technology & Innovation 22: 101491.
Syamsiro, M., Saptoadi, H., Norsujianto, T., Noviasri, P., Cheng, S., Alimuddin, Z. and Yoshikawa, K. 2014. Fuel oil production from municipal plastic wastes in sequential pyrolysis and catalytic reforming reactors, Energy Procedia 47: 180-188.
Wong, C., Yau, Y., Ong, H., and Chin, W. 2022. Study of climate change impacts on the lifespan of a bin weather data set in Senai, Malaysia, Urban Climate 44: 101219.

APPENDIX

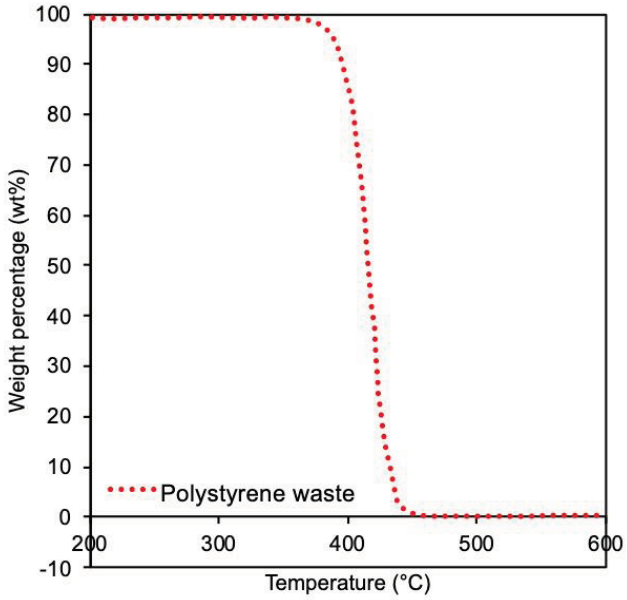

TGA curve of polystyrene plastic waste